Waste tyres valorisation through gasification in a bubbling fluidised bed: An exhaustive gas composition analysis

Daniel Serrano [a],[*], Alen Horvat [a], Esperanza Batuecas [a], Pedro Abelha [b]

[a] *Energy System Engineering Research Group, Thermal and Fluid Engineering Department, Carlos III University of Madrid, Leganés, Madrid, Spain*
[b] *Biobased and Circular Technologies, The Netherlands Organization for Applied Scientific Research (TNO), Petten, the Netherlands*

ARTICLE INFO

ABSTRACT

Waste tyres gasification in a bubbling fluidised bed reactor is evaluated by means of a complete characterisation of the product gas. The experiments are carried out at two temperatures, 700 and 850 °C, and various equivalence ratios (ER) while using air as a gasifying. Additionally, the effect of steam is also studied at 850 °C. High temperature and low ER increase the production of H_2, CH_4, and C_2H_4. Steam addition mainly affects H_2 and CO production. Low carbon conversion (CC) into gas and cold gas efficiency (CGE) are obtained, increasing with temperature and ER. The lower heating value (LHV) of the gas decreases with the ER because of the higher partial combustion rates. LHV values range between 12 MJ/Nm^3 with steam addition at ER = 0.13 and 850 °C to 5.3 MJ/Nm^3 at ER = 0.33 and 700 °C using air only. Along with a major permanent gas (CO_2, CO, H_2, CH_4, and C_2H_n), up to 25 short-chain hydrocarbons (non-aromatic hydrocarbons ranging from C_3 to C_{6+}) and two light aromatics are present in the product gas. Among short-chain hydrocarbons, C_3 and C_4 compounds are present in the highest yields. All these minor hydrocarbon species (i.e., C_3 to C_{6+}), not usually reported in biomass or waste gasification studies, yield up to 13 %vol. on a N_2-free basis. Their contribution to the gasification performance is important because they account for half of the energy content in the product gas. Therefore, it is important to consider them in the gasification process, not only for energy purposes but also for the chemical industry.

1. Introduction

Waste production is an issue of major concern for all governments as landfill capacities or legal permits are being severely reduced. Recently, the concept of circular economy is being integrated into waste treatment practices. The European Union (EU) is concerned about this problem, and it is promoting different actions to deal with it. The EU is addressing this problem with three EU directives. The Directive (EU) 2018/850 on the landfill waste points towards the reuse of materials to cover European needs [1]. The Directive (EU) 2018/851 on waste enforces a transition towards the circular economy, in which all residues are seen as by-products to be included again in the production process [2]. Finally, Directive (EU) 2018/852 on packaging and packaging waste promotes the minimisation of the use of packages by the use of reusable packaging [3]. All these normative attempt to avoid or reduce the negative environmental effects derived from landfilling. Reuse or valorisation is the best strategy to adopt the circular economy model. By 2035, only 10% of the residues can be disposed in landfills, which calls for specific actions to achieve this target.

The term waste is included in the definition of biomass, which is considered renewable energy. Accordingly, waste could be considered renewable energy as it derives from organic materials and is continuously generated. One of the residues widely produced is automobile tyres [4]. The European Tyre & Rubber Manufacturers Association (ETRMA) report states that 5.1 million tonnes of tyres were produced in 2018, 5 million tonnes in 2019 and 4.2 in 2020 [5]. Worldwide, global tyre production will increase from around 16000 to 23000 million tonnes from 2014 to 2024 [6]. An immense number of tyres becomes a problem at the end of their life as it would take thousands of years to decompose [7,8]. Table 1 shows the end-of-life tyres (ELT) management in 2019 for different European countries. The mean energy recovery value across these countries is close to 35%. Only Belgium, Denmark, Finland, Ireland, Malta and The Netherlands have a material recovery rate above 90% with very low energy recovery of the ELT. Nowadays, a small fraction of waste tyres is reused for second hand tyres while the rest is recycled into raw materials and valorised into energy. The rubber is mainly used in artificial grass for sports venues and safe playground floors, with a small contribution to the asphalt industries, thermal insulation and soundproofing. Regarding energy valorisation, ELT are

---

Nomenclature

Latin symbols

d_p	particle diameter [m]
D	reactor diameter [m]
g	gravity constant [m·s^{-2}]
h_b	bed height [m]
MW	molecular weight [g·mol^{-1}l]
$\dot{m}$	mass flow rate [kg·s^{-1}]
u_{mf}	minimum fluidisation velocity [m·s^{-1}]

Greek letters

ε	void fraction [−]
μ_g	dynamic viscosity of the fluidising agent [Pa·s]
ρ_{bulk}	bulk density of the solid particles [kg·m^{-3}]
ρ_g	density of the fluidising agent [kg·m^{-3}]
ρ_p	density of the solid particles [kg·m^{-3}]
σ_p	standard deviation of the particle size [m]
φ	sphericity of the solid particles [−]

Abbreviations

CC	carbon conversion
CGE	cold gas efficiency
ELT	end-of-life tyres
ER	equivalence ratio
FID	flame ionisation detector
GY	gas yield
ICP-AES	inductively coupled plasma atomic emission spectroscopy
LHV	lower heating value
PAH	polycyclic aromatic hydrocarbons
TCD	thermal conductivity detector

Table 1
End-of-life tyres (ELT) data for 2019 (Europe) [11].

Country	New tyres in the market [tonns]	Total material recovery [%]	Energy recovery [%]
Austria	74000	62.2	37.8
Belgium	81325	92.4	2.6
Bulgaria	40800	63.7	3.7
Croatia	26307	75.7	5.2
Cyprus	6900	36.2	108.7
Czech Rep.	93037	36.8	35.3
Denmark	49900	95.8	0.0
Estonia	13107	80.8	24.5
Finland	61060	110.6	9.8
France	422579	52.6	52.8
Germany	434000	68.0	31.6
Greece	45200	66.3	30.6
Hungary	44000	68.2	21.6
Ireland	32601	96.8	3.2
Italy	384000	44.5	44.3
Latvia	12500	64.0	28.0
Lithuania	21533	66.9	17.4
Luxembourg	0		
Malta	2300	100.0	0.0
The Netherlands	87746	91.1	8.9
Poland	268500	47.3	31.3
Portugal	72421	65.2	42.7
Romania	51413	1.1	98.9
Slovakia	27475	82.5	2.3
Slovenia	27307	27.5	48.2
Spain	238080	66.5	33.5
Sweden	93532	29.5	70.5
UK	452659	35.3	61.3
Norway	66620	30.3	71.2
Serbia	50000	78.0	22.0
Switzerland	47200	1.3	98.7
Turkey	227509	57.0	30.3
Total	*3555611*	*55.0*	*40.2*

used in energy demanding industries such as cement, steel, lime, and brick factories, as well as for power generation [8,9]. Since the material recovery cannot absorb all the ELT, energy recovery is an essential option to close the tyres cycle [10].

One of the main problems in waste tyres conversion for energy purposes is pollutant control in terms of sulphur, polycyclic aromatic hydrocarbons (PAH), and heavy metals [12]. The decomposition of polymers in the tyres is associated with the evolution of H_2S, COS, and other sulphur-containing gas species [13]. Thus, direct combustion of waste tyres should be avoided. Thermochemical conversion through pyrolysis and gasification is a feasible option to recover energy and raw

materials. These technologies enable better control of pollutants, and they also enable the utilisation of the produced gas for other applications than heat and power. The gas can be easily transported through pipes to wherever it is required. Gasification takes place at a lower temperature compared to combustion. This results in lower emissions of NO_x and SO_x. The gasification gas is also denser with a higher concentration of contaminants, making their removal as well as CO_2 capture more efficient compared to combustion gas [14–16]. Thus, the produced gas could be stored with no contaminants, avoiding their release into the environment.

Raman et al. were one of the pioneers in gasification of tyres [17]. They used steam and combustion exhaust gases as gasifying agents. H_2 yield increased with temperature while light hydrocarbons such as CH_4 and C_2H_n decreased. However, the experimental conditions were not explained in detail. Lee et al. used conditions close to pyrolysis but with an equivalence ratio (ER) in the range from 0 to 0.11 [18]. Marginal differences in the lower heating value (LHV) were obtained as the temperature varied from 700 to 880 °C. Leung and Wang employed air and steam in a fluidised bed gasifier to evaluate the effect of the ER and temperature [19,20]. They included compounds up to C_4 in the product gas composition. However, the temperature range was rather low for a gasification process (i.e., below 650 °C). Galvagno et al. gasified different materials, including tyres, in a rotary kiln using steam [12]. They obtained the highest hydrogen content (51.5 %vol.) and energy content (25.33 MJ m^{-3}) in the product gas when using tyres as feedstock. Relatively high production of methane (27.6 %vol.) and unsaturated C_2 compounds (9.9 %vol.) were also measured. Karatas et al. carried out a thorough product analysis of tyres gasification, testing mixtures of CO_2/air, air/steam, air, and steam as gasifying agents for different ER, temperatures, and bed particle sizes [21,22]. These studies focused on the LHV of the product gas considering the main gas compounds (CO_2, CO, CH_4, H_2, and O_2). Xiao et al. operated an air bubbling fluidised bed gasifier between 400 and 800 °C [23]. They concluded that low temperature gasification is more attractive to recover energy and materials such as carbon black from waste tyres. Conesa et al. performed the most complete gas analysis for tyre gasification in terms of the number of gaseous compounds (16 short-chain hydrocarbons and light aromatics) as well as 36 condensable species [24]. Recently, Esmaeili et al. gasified different solid wastes, including tyres. Waste tyres was the residue with the highest gas production [25]. Ongen et al. used an up-draft fixed bed reactor, obtaining a gas yield below 40 wt% [7].

In this work, the gasification of waste tyres is carried out in an atmospheric fluidized bed reactor working under autothermal conditions. Three sets of experiments are performed: (i) at low temperature (700 °C), (ii) at high temperature (850 °C) and (iii) at high temperature with steam addition. Along with that, ER in the range from 0.13 to 0.33

is tested for the two temperatures to evaluate the product gas and the gasification performance. Biomass and waste gasification studies are usually focused on the major gas species: CO_2, CO, H_2, and CH_4, to evaluate the potential use of the product gas as a fuel. Considering that little information about a complete gas composition and its influence on the energy content of the product gas, complete gas analysis is carried out. 25 different short-chain hydrocarbons, from C_3 to C_6, two light aromatics and heavier hydrocarbons grouped as C_{6+} are reported here. This is novel information since it is rarely reported in the existing literature. The knowledge of a complete gas analysis could provide alternative valorisation routes for the chemical industry. Including complete gas analysis into the gasification performance parameters will give better perspectives on the overall process.

2. Experimental setup

2.1. Materials

Waste tyres are used as feedstock to assess the gasification process as a valorisation route for this type of waste. Metallic wires are removed, and the material is chopped into small pieces of approximately 5 mm. A complete characterisation of the fuel is given in Table 2. Characterisation is carried out according to the following standards. Elemental analysis (NEN-EN-ISO 16948), moisture content (NEN-EN-ISO 18123), ash content determined at 815 °C (NEN-EN-ISO 18123), volatile matter (NEN-EN-ISO 18123), ash inorganic composition determined by ICP-AES (NEN 6966) after digestion with nitric acid, hydrofluoric acid, and perchloric acid for the determination of selected elements in solid matrices (NEN 6963), and higher heating value (NEN-EN-ISO 18125). The proximate and elemental analyses agree with the values reported by Karatas et al. [22] and Leung and Wang [20].

Silica sand is used as bed material for the fluidised bed reactor as it is the reference material in most of the gasifiers. The particle size of the bed material is characterised using different sieves with a mesh size between 150 and 600 μm. A Gaussian fitting from the experimental measurement gives a mean particle size value, d_p, of 376 μm and a standard deviation, σ_p, of 59 μm. Considering the size and density of the particles (ρ = 2439.1 ± 141.2 kg·m^{-3}, ρ_{bulk} = 1302.1 ± 30.2 kg·m^{-3}), they are classified as a type B material according Geldart's classification [26]. The minimum fluidisation velocity, u_{mf}, is estimated using the Carman-Kozeny correlation expressed by Eq. (1) [27]:

$$u_{mf} = \frac{(\varphi d_p)^2 (\rho_p - \rho_g) g}{180 \mu_g} \frac{\varepsilon^3}{1 - \varepsilon} \qquad (1)$$

where u_{mf} is the minimum fluidisation velocity, ρ_p and φ are the density and the sphericity of the solid particles, respectively, d_p is the particle diameter, ρ_g and μ_g are the density and the dynamic viscosity of the fluidising agent, respectivley, g is the gravity acceleration and ε is the void fraction. Since the minimum fluidisation velocity also depends on the temperature, this parameter is accounted for in the fluidising agent properties, ρ_g and μ_g [28]. Several values for u_{mf} are measured at different temperatures (23–600 °C) by visual inspection of the bed surface, detecting the time bubbles appear at the bed surface for the fluidization step and detecting the time bubbles disappear from the bed surface for the defluidisation step. This methodology minimises the effect of cohesion forces between bed particles. The sphericity of the particles is determined from the fitting of the experimental data as a free parameter. The estimation of the minimum fluidisation velocity, according to the Carman-Kozeny equation results in a value of u_{mf} = 5.64 and 5.12 cm·s^{-1} for 700 °C and 850 °C, respectively, with particle sphericity φ = 0.80.

2.2. Experimental facility

Experiments are performed in a lab-scale biomass fluidised bed research facility (WOB) previously used not only for gasification purposes but also for pyrolysis and combustion with different types of fuels and residues [29]. The WOB gasifier is an air-blown fluidised bed reactor electrically heated and thermally insulated with an inner diameter in the bed section of 77.9 mm and a length of 450 mm from the distributor plate. The upper part of the reactor (freeboard) has a wider inner diameter (102.3 mm) and a length of 905 mm. In the freeboard, the gas velocity is reduced which also reduces entrainment of the bed particles. The raw gas produced in the reactor passes through a hot cyclone to remove carryover particles. The gas is finally sent to an afterburner which burns the gas before it is released into the atmosphere. The facility is equipped with several sampling points for gas and tar analyses, although only the port located after the hot cyclone is used in this work. These arrangements make it possible to study how the gas species react along the reactor (i.e., from the bed to the facility outlet). Thus, a design of the gasifier can be adjusted according to the desired gas composition. A scheme of the experimental facility is presented in Fig. 1. The WOB facility is instrumented with several thermocouples and pressure sensors to monitor the process. The signals are acquired and saved every 10 s.

The feeding system, with a feeding capacity of approximately 1 kg·h^{-1}, is composed of a hopper for the tyre material and two screw feeders: the first one to control the fuel feeding rate, and the second one to quickly introduce the fuel into the gasifier. The two screw feeders are positioned one on top of the other. Tyres are fed into the reactor 30 mm above the distributor plate.

Table 2
Characterisation of waste tyres.

Proximate analysis [wt.% ar]		Elemental analysis [wt.% db]		Inorganics [mg·kg^{-1} db]			
Moisture	1.19 ± 0.13	Carbon	74.75 ± 3.00	Al	1547.09	Mn	33.17
Volatile	64.76 ± 0.85	Hydrogen	5.46 ± 1.06	As	<2	Mo	<1
Fixed Carbon[a]	25.19 ± 1.47	Nitrogen	0.71 ± 0.19	B	10.64	Na	460.20
Ash	8.86 ± 1.84	Sulphur	1.15 ± 0.20	Ba	13.26	Ni	5.82
		Oxygen[a]	8.96 ± 3.80	Br	489.00	P	179.00
				Ca	4507.28	Pb	23.62
Higher Heating Value [MJ·kg^{-1} ar]			35.11 ± 1.39	Cd	0.77	Sb	5.48
				Cl	643.00	Se	<2
				Co	181.38	Si	32317.55
				Cr	5.99	Sn	3.52
				Cu	374.37	Sr	4.39
				F	21.00	Ti	80.51
				Fe	4906.56	V	3.03
				K	545.49	W	4.49
				Li	2.27	Zn	17842.34
				Mg	669.35	Hg	0.02

ar: as received, db: dry basis, [a] determined by difference.
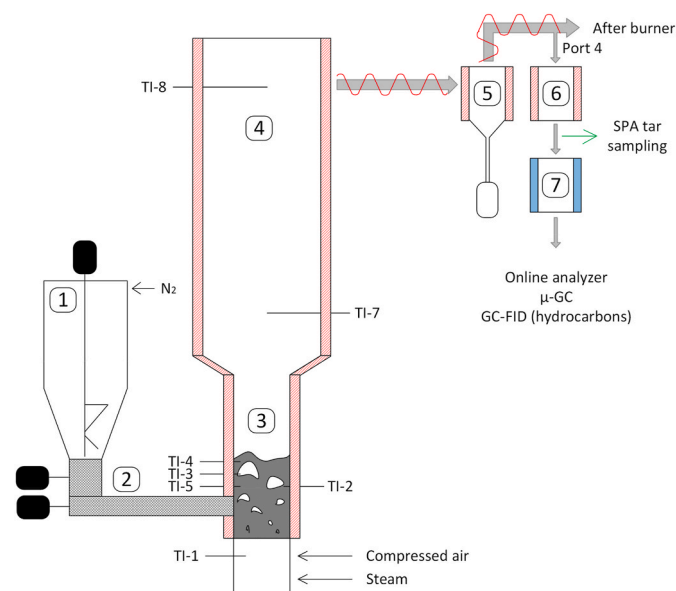
Fig. 1. Schematic diagram of WOB facility: (1) feedstock hopper; (2) screw feeders; (3) BFB reactor; (4) freeboard; (5) hot cyclone; (6) hot filter; (7) cleaning section.

2.3. Experimental procedure

The reactor is loaded with 900 g of silica sand, resulting in a bed aspect ratio of $h_b/D = 1.86$ ($h_b = 145$ mm). The electrical elements heat the bed to the desired temperature (700 or 850 °C) while the air supply is set to the experimental value according to the ER. Table 3 shows the experimental conditions tested. Additionally, extra N_2 (2 Ndm^3·min^{-1}) is introduced in the feeding system to avoid backflush of the produced gases into the hopper. In some cases, additional N_2 is added in the plenum in order to maintain the fluidization regime. Mass flows are precisely adjusted by mass flow rate controllers. Once the desired temperature is reached, the acquisition of temperature and pressure signals as well as the feeding system is started. Because of the experimental conditions and the facility characteristics, the final reactor temperature is adjusted by switching off the electrical furnaces. When gas composition and temperature profiles are stable, the gas and tar samples are taken. Gasification tests are performed in endothermic mode as air is used as gasifying agent. Partial combustion of the tyres supplies the required energy for endothermal reactions in the reactor. The external energy input, supplied by the electrical heating elements, is not needed once the feeding is initiated. Consequently, the temperature and the ER cannot be adjusted separately as they are not independent. This is the reason why upon the change of ER values the bed temperature cannot be maintained. For example, when operating at a theoretical reaction temperature of 700 °C and ER = 0.16, the actual temperature reached 690 °C while at ER = 0.33 the actual temperature reached 730 °C. This

operation mode is very important for waste treatment as the reaction is self-maintained without external energy requirements despite the energy content in the product gas is reduced due to the nitrogen dilution.

The experiments from #06 to #08 (Table 3), are carried out using a steam addition of 150 g·h^{-1} which gives a steam-to-fuel mass ratio of 0.39. Steam is produced by a steam generator, and it is mixed with the inlet air and N_2 in the plenum chamber just before the distributor plate. Due to the steam addition, the amount of N_2 to maintain the fluidisation regime is reduced or not used at all. This set of experiments is performed at 850 °C and different ER.

2.4. Sampling and analysis

Prior to the gas analysis, the raw gas leaving the reactor passes through a cleaning section to remove fly ash, entrained particles from the bed, water, and tar. Firstly, fly ash and entrained particles are removed in a hot cyclone kept at 450 °C. The solids collected in this part of the installation are collected individually for the different experimental conditions and kept for a further analysis. Around 1 Ndm^3·min^{-1} of particle free gas is taken through the gas and sampling section while the rest was burned to fulfill safety and environmental regulations.

The stream destined for gas analysis passes through a hot filter (450 °C) and a condenser kept at 4 °C to condense water and tar compounds. Further cleaning takes place in an empty impinger bottle submerged in a water bath also at 4 °C. A HEPA filter is placed before the online analysers to remove the remaining aerosols. The remaining water content in the gas is finally reduced to a maximum value of 0.8%. Finally, the gas, now considered a dry gas, is analysed by an online gas analyser (ABB Optima) equipped with three detectors: (i) infrared detector to quantify CO_2, CO and CH_4; (ii) paramagnetic detector to quantify O_2; and (iii) thermal conductivity detector to measure H_2 content. These compounds are continuously recorded with a sampling rate of 0.1 Hz.

After leaving the online analysers, the gas is further analysed in 4 min intervals using a Varian μ-GC CP4900 equipped with 4 channels and a thermal conductivity detector (TCD) for the determination of permanent gases, C_2 light hydrocarbons, and light aromatic compounds. A Molsieve MS5 column is employed for the determination of Ne, N_2, CH_4, and CO. A PPU (Poraplot) column is used for the quantification of CO_2, C_2H_2, C_2H_4, and C_2H_6. Finally, a CP-Wax-52CV column is used for the measurement of benzene and toluene. These three columns are 10 m in length while using He as the carrier gas. Note that a small amount of Ne (0.02 Ndm^3·min^{-1}) is introduced in the reactor to calculate the total gas yield by monitoring a mass balance of this inert gas.

Additionally, some gas samples are also taken after the online gas analysers to measure other short-chain hydrocarbons which are not reported in the literature (i.e., C_3, C_4, C_5, C_6, and C_{6+}). Two gas bags are collected for each experimental condition. A first gas sample is taken at the beginning of each experimental condition, after the reactor is stabilised, and a second one after 30 min to check the concentration of the gas along the experiment. Short-chain hydrocarbons (see Fig. S1 in

Table 3
Operating conditions.

	#01	#02	#03	#04	#05	#06	#07	#08
Feeding rate [kg$_{ar}$·h^{-1}]	0.32	0.32	0.39	0.39	0.39	0.38	0.38	0.38
Air flow rate [Ndm^3·min^{-1}]	7.14	14.27	7.14	10.72	14.27	7.14	10.72	14.27
Additional N_2 [Ndm^3·min^{-1}]	10.05	5.80	10.03	7.35	3.80	3.87	1.05	–
Steam [kg·h^{-1}]	–	–	–	–	–	0.15	0.15	0.15
ER [−]	0.16	0.33	0.13	0.20	0.27	0.13	0.20	0.27
TI-1 [°C]	381.9	314.3	567.2	520.7	521.8	604.8	530.6	526.2
T_{bed} [°C][a]	687.2	732.3	843.3	846.4	850.6	847.1	855.6	860.2
TI-7 [°C]	690.6	651.9	818.9	774.5	769.7	769.7	760.9	747.5
TI-8 [°C]	664.8	646.0	732.0	638.5	675.6	599.0	594.2	595.2

[a] mean value between TI-2, TI-3, TI-4 and TI-5.

Supplementary information) are analysed by means of a GC (Thermo Quest CE Instruments Trace GC Ultra) coupled with a flame ionisation detector (FID). Chromatographic separation is carried out through an Al_2O_3/KCl capillary column (50 m × 0.32 mm x 5 μm) using He as the carrier gas for hydrocarbon determination. Gas sample injections are performed at constant volume (25 μl) and atmospheric pressure. Prior to injection, the sample loop is flushed by the sample for 2 min with a volume flow rate between 1 and 5 ml/min. The GC oven is programmed isothermally at 127 °C. The FID is set to 200 °C with an air flow rate of 350 ml/min, a H_2 flow rate of 35 ml/min and a makeup gas of 35 ml/min. The total acquisition time is 40 min. FID calibration is performed by means of a gas mix formed by several n-hydrocarbons ranging from C_3 to C_6. The detection limit for FID is 1 ppm.

The analysis of gasification performance includes gas LHV, carbon conversion into a gas (CC), and cold gas efficiency (CGE). LHV is calculated using Eq. (2) [16]. It considers the gas composition ($[\%vol.]_i$) and the LHV (LHV_i) of each gas compound detected after the gas cleaning section. The LHV of each gas compound can be found in the Supplementary information. CC (Eq. (3)) represents the ratio of carbon

mass flow rate in the dry, tar-free product gas ($\sum_{i,C\ species} \dot{m}_i \cdot \frac{MW_C}{MW_i}$) to the mass flow rate of carbon in the dry and ash-free biomass ($\dot{m}_{fuel} \cdot [\% C]_{fuel}$). Only carbon-containing species in the gas are considered for calculation of the CC value. CGE defined by Eq. (4) is the energy output ($LHV_{gas} \cdot GY$) over the potential energy input ($\dot{m}_{fuel} \cdot LHV_{fuel}$) [30].

$$LHV = \sum_i LHV_i \cdot [\%vol.]_i \qquad (2)$$

$$CC = \frac{\sum_{i,C\ species} \dot{m}_i \cdot \frac{MW_C}{MW_i}}{\dot{m}_{fuel} \cdot [\% C]_{fuel}} \qquad (3)$$

$$CGE = \frac{LHV_{gas} \cdot GY}{\dot{m}_{fuel} \cdot LHV_{fuel}} \qquad (4)$$
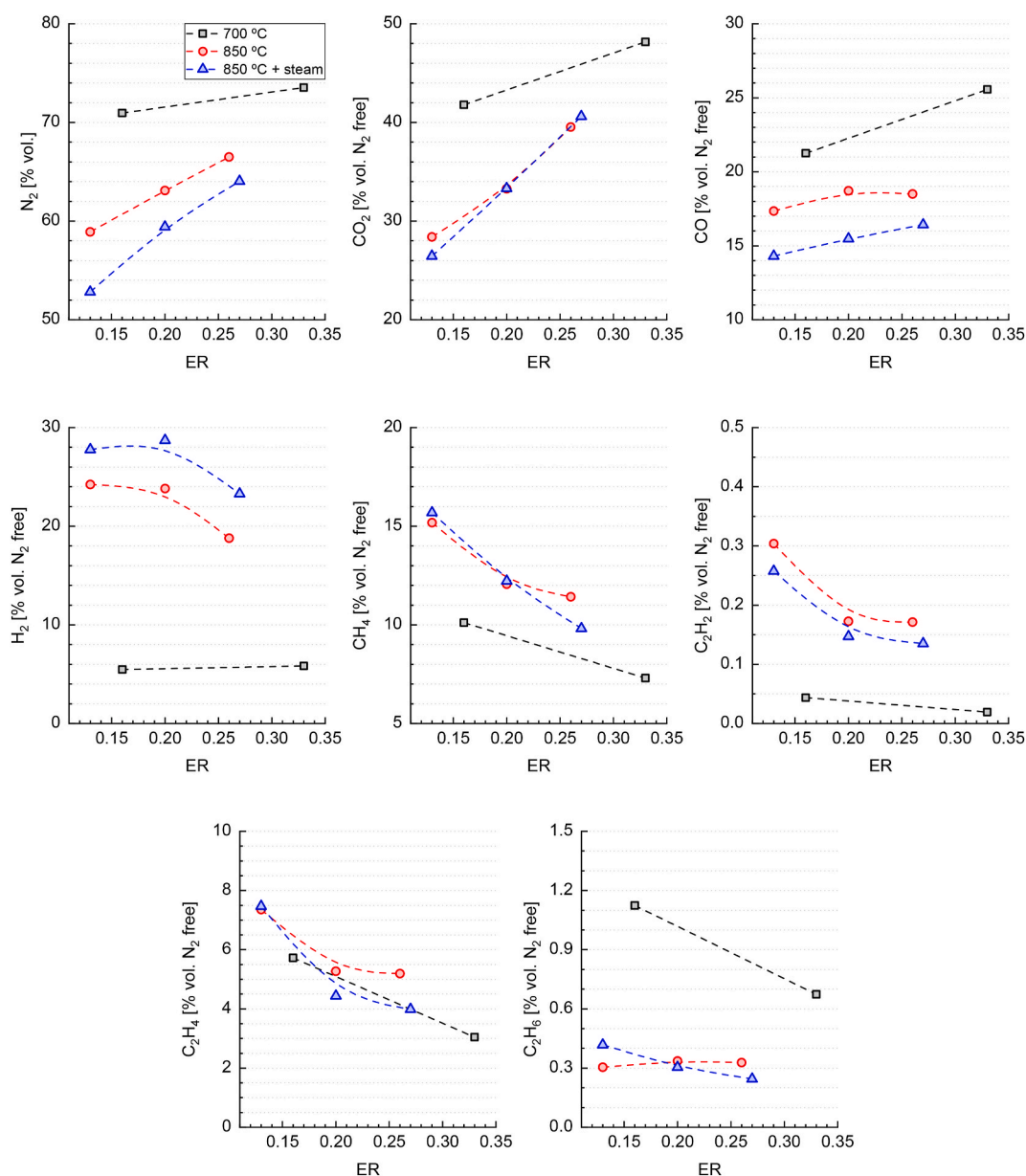
Fig. 2. Yields of major gas species and light hydrocarbons.

3. Results and discussion

3.1. Effect of the ER and temperature on the product gas composition

The product gas composition is given as a function of the ER for two different temperatures: low (700 °C) and high (850 °C) temperature. The gas is composed of major compounds such as CO_2, CO, H_2, CH_4, C_2H_2, C_2H_4, C_2H_6, and N_2, and minor hydrocarbons ranging from C_3 to C_{6+}. The ER is adjusted by modifying the air flow rate and, consequently, the N_2 flow introduced in the plenum to keep a consistent fluidisation regimen throughout all tests. The gas composition is expressed in a N_2-free basis to facilitate the comparison of the results between test conditions as well as with the literature data.

Fig. 2 shows the gas composition measured at the exit of the WOB facility. An increase in the air flow rate also increases yields of CO_2 and CO. At a temperature of 700 °C, the ER = 0.33 delivers a higher CO_2 yield by an absolute value of 6.4 %vol. compared to the ER = 0.16. In the case of CO yield, a slightly lower increase by 4.6 %vol. absolute is observed due to the ER change. H_2 concentration remains rather constant regarding the ER change. A marginal increase of 0.3 %vol. absolute is observed between ER = 0.16 and 0.33. For both ER values at 700 °C, H_2 yields reach nearly 6 %vol. Other major gas compounds (i.e., CH_4 and C_2H_n) show a decreasing tendency with the increase of the oxygen input, due to higher oxidation rates. Yields of CH_4 and C_2H_4 decreased by 2.7 %vol. absolute. It is worth to mention that the production of C_2H_4 is in the same quantity range as H_2 while C_2H_6 and C_2H_2 are produced in small quantities, below 1 %vol.

The gas composition for the process conditions at 850 °C is also plotted in Fig. 2. In this set of experiments, three ER values are tested. With respect to the ER variations, the reactor temperature (Table 3) is relatively constant despite operating in an autothermal mode. This indicates that gasification is at the upper limit of autothermal conditions. The required energy for the gasification reactions and the thermal losses of the reactor would surpass the energy supplied by the tyres combustion at temperatures higher than 850 °C. Thus, additional external energy should be supplied. Between ER = 0.13 and 0.20 the increment of CO yield is small, only 1.4 %vol. absolute. CO yield remains constant between ER = 0.20 and 0.26. Up to 24.2 %vol. of H_2 is obtained for ER = 0.13 and 0.20 at 850 °C, but the yield declines with the further increase in ER. A similar diminution trend is observed for CH_4 and C_2H_4 although the reduction is sharper from low to medium ER. The effect of temperature on the yields of CH_4 and C_2H_4 is not as significant as it is for H_2. The yields of CH_4 and C_2H_4 remain similar at both temperatures. The production of C_2H_6 and C_2H_2 remains similar at both temperatures as well (i.e., below 1 %vol.).

Light hydrocarbon species in the gas are mainly produced by the breakdown of the tyre polymers (usually made of a styrene-butadiene heterodimer) and by secondary gasification reactions [31,32]. These reduced hydrocarbon chains are further cracked and oxidised into the major gas compounds. Several authors have reported secondary aromatisation reactions as the fundamental path for H_2 and CH_4 production [33,34]. The relevant C_2H_n concentrations (3.7–8.2 %vol.), in this study, are mainly formed by C_2H_4, which supports the results reported by Dodds et al. who stated that the high number of reactive radicals coming from the cleavage of butadiene C=C double bond are responsible for the presence of alkenes [32].

The evolution of the compounds presented in Fig. 2 is in close agreement with the literature data. However, Karatas et al. [22] obtained higher H_2 and CH_4 concentrations (on a N_2-free basis) while the yields of CO and CO_2 were lower. Xiao et al. [23] achieved similar CO, CO_2, H_2, and CH_4 yields but higher quantities of C_2H_n and C_mH_n. Lee et al. [18] also obtained a high concentration of C_2H_4, which is an interesting raw material for the chemical industry. However, the C_2H_4 yields obtained in the present study are comparable to H_2 production at low temperatures. The results reported by Karatas et al. [22] should be considered carefully because the effect of ER is decoupled from the effect

of temperature. Note that in the present work, in low temperature range, the temperature between ER = 0.16 and 0.33 also varies by 50 °C, due to the autothermal gasification mode. At high temperature, H_2 also decreases with ER, being the temperature constant for the range of ER studied, and the concentrations are close to those reported in by Karatas et al. [22]. Wang and Leung [19] performed tests at lower temperature and ER, achieving quite different results, with high CO and C_2H_6 concentrations. This is contrary to the results obtained in this study and the corresponding literature [22,23]. Most of the divergences observed between these diverse studies can be attributed to differences in the fuel composition, temperature, and ER conditions, but also to the different residence times used.

The temperature has an important effect on the gas composition with a notable difference in the H_2 production, from ~6 %vol. at 700 °C to ~22 %vol. at 850 °C. CH_4 and C_2H_2 also experience a small increase while C_2H_6 and C_2H_4 show a slight reduction. Higher temperature promotes thermal cracking reactions of alkanes into H_2 and CH_4. This observation was also reported by Li et al. [35] for plastic waste gasification. CO_2 concentration is reduced at elevated temperature due to the endothermicity of the CO_2 reforming reactions which are enhanced at high temperatures [36] and could promote the production of H_2.

Apart from the major permanent gas species, 25 short-chain hydrocarbons, 2 light aromatics, and compound group C_{6+} are also measured. Compound group C_{6+} accounts for hydrocarbons with six or more C atoms. C_{6+} hydrocarbons are not separated in the chromatographic column and they are accounted all together. Fig. 3 shows that significant quantities of C_3 and C_4 compounds are produced at low temperatures. Propylene is the main C_3 compound while 2-butyne, 1,3-butadiene, and 1-butene are the main C_4 species. The yields of short-chain hydrocarbons are given in the Supplementary information (Table S1). The presence of C_5 and C_6 compounds is marginal. Around 0.3 %vol. for C_5 and less than 0.01 %vol. for C_6. Heavier hydrocarbons (C_{6+}) and light aromatics like benzene and toluene are produced in concentrations between 1 and 3 %vol. Similarly to light hydrocarbons (i.e., C_2), a decrease in their concentration is observed at the highest ER for all C groups. At high temperature, 850 °C, C_3, C_4, and C_6 experiences an increase from ER = 0.13 to 0.20, followed by a slight decrease at ER = 0.26. Now the main groups produced under high temperature conditions are C_{6+}, benzene, and toluene. In general terms, the increase in the temperature reduces the total short-chain hydrocarbons down to approximately 6 %vol. while the lighter gas species increase. According to Larsgoiti et al. [31], the formation of C_4 and C_{4+} takes place in the early stages of tyre devolatilisation as a consequence of thermal degradation. Due to the presence of styrene in the original tyre, the formation of benzene and toluene is derived from styrene decomposition [32].

Short-chain hydrocarbons and light aromatics are usually not reported in the literature due to their low concentrations, in the range of ppm_v, or due to inadequacy of measurement protocols. However, these compounds are relevant. In the present study, they account for 13.4 %vol. (on N_2 free basis) of the total gas composition, for ER = 0.16 and around 8.8 %vol. for ER = 0.33 at low temperature. Their contribution at high temperature is approximately 6 %vol. Therefore, their presence has an important effect on the LHV of the product gas. Previous studies reported a total yield of C_mH_n, grouped up to C_4 [18–20] or $C_{1-8}H_n$ [23]. Conesa et al. [24] reported a list of short-chain hydrocarbons and light aromatics, similar to the present study. They reported 13 short-chain hydrocarbons in the range from C_3 to C_5. However, the temperature and ER values are not comparable as they operated at a low ER (0.10). Propylene was reported as the main C_3 compound while 1,3-butadiene and 1-butene were the main C_4 compounds, which agrees with the results of the present study.

Even though the two sets of tests performed at low and high temperatures, have different ER, some comparison could be carried out. The effect of N_2 dilution is reduced when the temperature is increased due to higher production of H_2 (from 5.5 to 22.2 %vol., approximately) and a moderate increase in CH_4 (8.7 vs. 12.9 %vol., approximately), given on
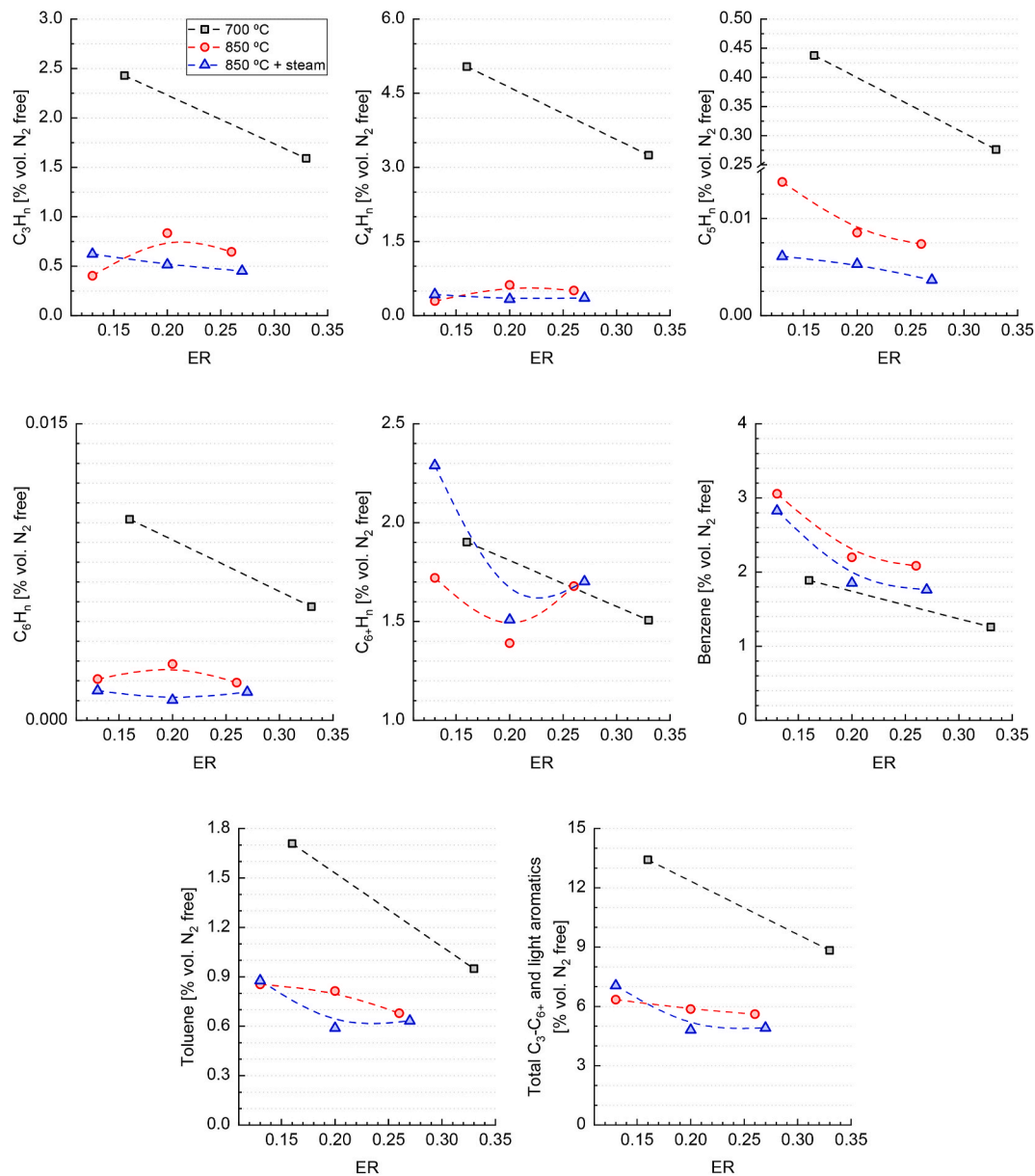
Fig. 3. Yields of short-chain hydrocarbons and light aromatics.
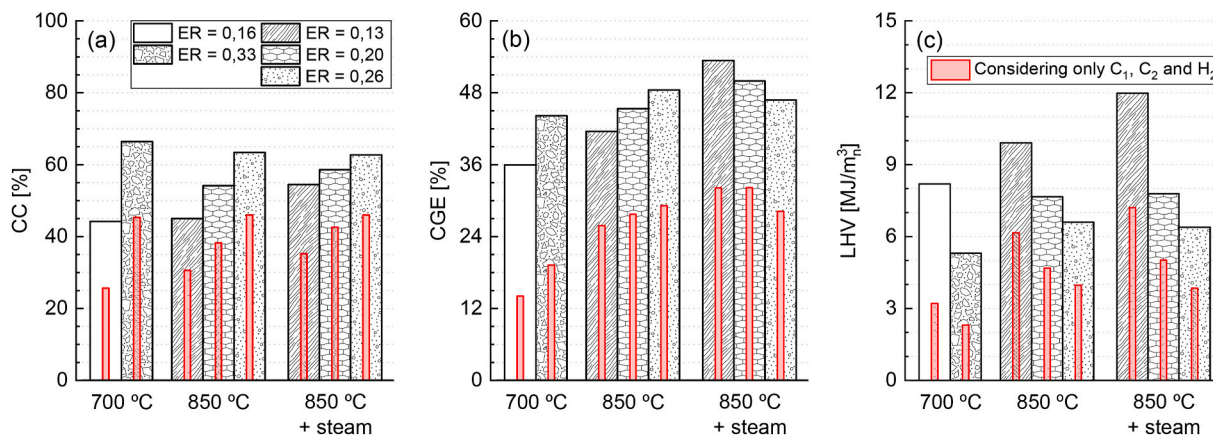
Fig. 4. Gasification performance: (a) carbon conversion (CC), (b) cold gas efficiency (CGE), and (c) lower heating value (LHV).

N_2-free basis. The effect of temperature on the gasification process is crucial for the production of different gas species. Light hydrocarbons such as C_2H_4 and C_2H_2 also experience an increase with temperature. As stated earlier, the yields of all short-chain hydrocarbons are reduced with the effect of the temperature, being C_3 and C_4 the most affected groups. These effects suggest the thermal cracking of short-chain hydrocarbons into lighter gas compounds such as H_2, CH_4, and C_2H_n.

3.2. Gasification performance

Gasification performance is evaluated in terms of carbon conversion into a gas (CC), cold gas efficiency (CGE), and LHV of the product gas. Fig. 4 shows that the CC and the CGE increase with ER at 700 °C. However, both CC and CGE values are rather low, between 44 and 66% for CC, and 36 and 44% for CGE, for ER = 0.16 and 0.33. The low CC is explained by the amount of entrained char particles collected in the cyclone. CC and CGE values are similar to those reported in the literature for CO_2 assisted gasification of tyres [36] and plastic wastes [35]. The CGE is in close relation with the LHV and the gas yield (GY). The LHV decreases from 8.2 $MJ \cdot Nm^{-3}$ to 5.3 $MJ \cdot Nm^{-3}$ as a consequence of the higher oxidation rates and thus, higher CO_2 concentration in the product gas. These are moderate LHV values despite the relatively high N_2 dilution (i.e., between 53 and 73 %vol.). GY increases with ER (see Table S1 Supplementary information). The parameters of gasification performance with respect to ER follow similar trends at high temperature. The CC, CGE, and LHV are improved with the increase in temperature due to the higher production of H_2, CH_4, C_2H_n, and benzene which contributes to a higher LHV. Additionally, CO_2 decreases with temperature. At this point, the reader must keep in mind the differences in the ER for both 700 and 850 °C. Hypothetically, a gasification test operated at ER = 0.16 and 850 °C would deliver a CC around 49%, which is 6.7% higher than CC associated to test conditions ER = 0.16 and 700 °C. In the same way, the CGE and LHV would improve by 7.2% and 0.75 $MJ \cdot Nm^{-3}$, respectively from 700 to 850 °C. The same calculations for a hypothetical test operated at ER = 0.23 and 750 °C would result in a 3.12% higher CC, a 4.54% higher CGE, and 1.16 $MJ \cdot Nm^{-3}$ higher LHV, compared to the case of 850 °C.

As previously stated, the inclusion of short-chain hydrocarbons and light aromatics makes a difference in the CC, CGE, and LHV as it is shown by the thin red bars in Fig. 4. Thin red bars account only for H_2, C_1, and C_2 species. The LHV of each short-chain hydrocarbon (see Supplementary information, Table S2) is between 2 and 15 times higher than the LHV of major gas species (i.e., H_2, C_1, and C_2). The LHV of the gas is calculated based on the compounds that remained in the gas after the cleaning section. A fraction of the C_5, C_6, and C_{6+} will condensate as their boiling point is above the temperature used in the cleaning section. Despite its low concentration, short-chain hydrocarbons and light aromatics have an impact on the energy content of the gas. This aspect is very important if combustion is the final use of the gas. Looking at the results, around half of the LHV and the CC values attribute to the short-chain hydrocarbons and light aromatics. Therefore, gasification parameters reported in the literature would improve by considering these extra gas species. The CGE values excluding short-chain hydrocarbons and light aromatics are in line with literature data (in the range of 10–36%) [18–20]. The effect of N_2 dilution in the present study delivers a product gas with a LHV lower than 40 $MJ \cdot Nm^{-3}$ as previously reported by Xiao et al. [23]. Karatas et al. [22] and Leung and Wang [20] obtained similar LHV values to those obtained in this study.

3.3. Steam gasification

In order to investigate the effect of steam on the gasification process, three experiments are performed at high temperature (850 °C) with a steam-to-fuel ratio of 0.39. Fig. 2 shows the results of the gas composition for the three different ER. Similar trends in the individual gas species are observed between the tests with and without steam.

Generally, the major gas compounds remain consistent with regard to the tests performed at 850 °C with no steam addition. However, there is a difference in H_2 and CO content because steam is the main H_2 source in addition to the temperature effect [35]. Measured H_2 yields are between 3.6 and 4.9 %vol. absolute greater when steam is added in the reactor while CO is reduced by around 3 %vol. absolute. The increase in the H_2 and the decrease in the CO indicate the importance of the water gas shift reaction and steam reforming reactions. Steam addition results in a slight decrease of light (C_2H_n) and short-chain hydrocarbons (C_3 to C_{6+}) as well as light aromatics (benzene and toluene). Additionally, H_2 can be produced from the dehydrogenation of light and short-chain hydrocarbons (C_2 to C_6) as recently reported by Xuan et al. [37].

The total concentration of short-chain and light aromatics hydrocarbons is reduced as the ER increases, in the same way as in the sets of experiments at 700 and 850 °C with no steam addition (Fig. 3). At low ER, a slight increase (0.7 %vol. absolute) in the total concentration is observed compared to the tests with no steam addition. C_3, C_4, and C_{6+} hydrocarbons increase marginally, but benzene suffers a decrease. At mid and high ER values, the total concentration stabilises close to 5 % vol., which is the lowest value in this experimental campaign. Benzene and C_{6+} are the main short-chain hydrocarbons and aromatics with approximate yields of 2 %vol. This is in line with the test without steam addition. The concentrations of toluene and propylene are between 0.4 and 1 %vol. The use of steam reduces the short-chain hydrocarbons and light aromatics as a consequence of steam reforming reactions [38].

In Fig. 4 the steam addition is evaluated with respect to gasification performance. At low ER, the CC value increases with the addition of steam. However, this improvement reduces at further increases in ER due to the reduction of carbon-containing species. Both CGE and LHV values show improvements with steam addition due to the higher H_2, CH_4, and C_{6+} production. An increase in the LHV is also observed by Wang and Leung [19], who reported changes from 6 to 10 $MJ \cdot Nm^{-3}$. Improvement in the energy content of the product gas is a consequence of the previously mentioned H_2 in particular. However, reduced concentration of the gas species with ER results in a decrease in LHV value. Despite this reduction, the steam addition is profitable for the gasification process [39].

4. Conclusions

Automotive tyres, a harmful waste is gasified in a bubbling fluidised bed reactor to evaluate its potential in terms of gas composition. Gasification tests are conducted at different temperatures and equivalence ratios while a set of tests is carried out with steam addition. Higher temperatures promote higher yields of key gas species such as H_2, CH_4, and C_2H_4, while reducing N_2 dilution and CO concentration. This effect is more pronounced at low ER values. The steam addition results in noticeably higher H_2 production and lower CO concentration. The gasification performance is rather low with low values of CC and CGE compared to biomass feedstocks.

Up to 25 short-chain hydrocarbons are measured and reported. The measurement of these species reveals their importance to the final product gas composition as they account for a high volumetric fraction as well as energy content. This aspect modifies the composition and characteristics of the final product gas. In this study, the amount of short-chain hydrocarbons ranges from 5 to 13 %vol. on a N_2 free basis. Short-chain hydrocarbons account for half of the product gas LHV, reaching 11.97 $MJ \cdot Nm^{-3}$. Typical gasification results already reported in the literature might improve if the contribution of these compounds is accounted for.

This study should also consider the sulphur-containing compounds produced in the waste tyre gasification process because sulphur is toxic to living organisms, deteriorates exposed materials in process installations, and deactivates reforming catalysts. In this context, future works should focus on the fate of sulphur in both gas phase and tar.

CRediT authorship contribution statement

Daniel Serrano: Conceptualization, Methodology, Investigation, Writing – original draft, Writing – review & editing. **Alen Horvat:** Conceptualization, Methodology, Investigation, Writing – review & editing. **Esperanza Batuecas:** Investigation, Writing – review & editing. **Pedro Abelha:** Methodology, Investigation, Writing – review & editing.

Declaration of competing interest

The authors declare that they have no known competing financial interests or personal relationships that could have appeared to influence the work reported in this paper.

Acknowledgement

Appendix A. Supplementary data

Supplementary data to this article can be found online at https://doi.org/10.1016/j.renene.2022.10.025.

References

[1] European Parliament, Directive (EU) 2018/850 of the European Parliament and of the Council of 30 May 2018 Amending Directive 1999/31/EC on the Landfill of Waste, 2018. http://data.europa.eu/eli/dir/2018/850/oj.

[2] European Parliament, Directive (EU) 2018/851 of the European Parliament and of the Council of 30 May 2018 amending Directive 2008/98/EC on waste, http://data.europa.eu/eli/dir/2018/851/oj, 2018.

[3] European Parliament, Directive (EU) 2018/852 of the European Parliament and of the Council of 30 May 2018 Amending Directive 94/62/EC on Packaging and Packaging Waste, 2018. http://data.europa.eu/eli/dir/2018/852/oj.

[4] R. Cossu, T. Lai, Automotive shredder residue (ASR) management: an overview, Waste Manag. 45 (2015) 143–151, https://doi.org/10.1016/J.WASMAN.2015.07.042.

[5] European Tyre, Rubber Manufactures Association, The ETRMA Statistics Report, 2021. https://www.etrma.org/wp-content/uploads/2019/10/20191114-Statistics-booklet-2019-Final-for-web.pdf.

[6] J. Young, New Technologies Improve Efficiencies amid Industry Evolution, Tyre Review, 2019. https://www.tirereview.com/tire-manufacturing-trends-new-technologies-improve-efficiencies-amid-industry-evolution/. (Accessed 26 July 2022).

[7] A. Ongen, H.K. Ozcan, E. Elmaslar Ozbas, Y. Pangaliyev, Gasification of waste tires in a circulating fixed-bed reactor within the scope of waste to energy, Clean Technol. Environ. Policy 21 (2019) 1281–1291, https://doi.org/10.1007/S10098-019-01705-0/TABLES/8.

[8] S.A. Ecoelastika, Annual Report, 2020.

[9] Sistema Colectivo de Gestión de Neumáticos Fuera de Uso, Annu. Rep. (2020) 2020.

[10] Ecopneus, 10 Years of Commitment and Results for the Italian Circular Economy, 2020.

[11] European Tyre and Rubber Manufactures Association, In Europe 95% of All End of Life Tyres Were Collected and Treated in 2019, 2021.

[12] S. Galvagno, G. Casciaro, S. Casu, M. Martino, C. Mingazzini, A. Russo, S. Portofino, Steam gasification of tyre waste, poplar, and refuse-derived fuel: a comparative analysis, Waste Manag. 29 (2009) 678–689, https://doi.org/10.1016/J.WASMAN.2008.06.003.

[13] H. Hu, Y. Fang, H. Liu, R. Yu, G. Luo, W. Liu, A. Li, H. Yao, The fate of sulfur during rapid pyrolysis of scrap tires, Chemosphere 97 (2014) 102–107, https://doi.org/10.1016/J.CHEMOSPHERE.2013.10.037.

[14] U.S.D. of E. National Energy Technology Laboratory, Emissions advantages of gasification, n.d. https://netl.doe.gov/research/coal/energy-systems/gasification/gasifipedia/low-emissions. (Accessed 22 July 2022).

[15] J.A. Ruiz, M.C. Juárez, M.P. Morales, L.M. López-Ochoa, J. Doménech, Biomass gasification or combustion for generating electricity in Spain: review of its current situation according to the opinion of specialists in the field, J. Renew. Sustain. Energy 5 (2013), 012801, https://doi.org/10.1063/1.4792605.

[16] P. Basu, Biomass Gasification and Pyrolysis, Elsevier Inc., 2010, https://doi.org/10.1016/C2009-0-20099-7.

[17] K.P. Raman, W.P. Walawender, L.T. Fan, Gasification of waste tires in a fluid bed reactor, Conserv. Recycl. 4 (1981) 79–88. https://www.sciencedirect.com/science/article/pii/0361365881900369. (Accessed 26 December 2021).

[18] J. Min Lee, J. Soo Lee, J. Rae Kim, S. Done Kimt, Pyrolysis of waste itres with partial oxidation in a fluidized-bed reactor, Energy 20 (1995) 969–976.

[19] C.L. Wang, D.Y.C. Leung, Characteristics of Tyre Powder Gasification Using a Fluidized Bed with Air/steam Mixture, Sustainable Energy and Environmental Technologies, 2000, pp. 247–251, https://doi.org/10.1142/9789812791924_0044.

[20] D.Y.C. Leung, C.L. Wang, Fluidized-bed gasification of waste tire powders, Fuel Process. Technol. 84 (2003) 175–196, https://doi.org/10.1016/S0378-3820(03)00054-7.

[21] H. Karatas, H. Olgun, F. Akgun, Experimental results of gasification of waste tire with air&CO2, air&steam and steam in a bubbling fluidized bed gasifier, Fuel Process. Technol. 102 (2012) 166–174, https://doi.org/10.1016/J.FUPROC.2012.04.013.

[22] H. Karatas, H. Olgun, B. Engin, F. Akgun, Experimental results of gasification of waste tire with air in a bubbling fluidized bed gasifier, Fuel 105 (2013) 566–571, https://doi.org/10.1016/J.FUEL.2012.08.038.

[23] G. Xiao, M.J. Ni, Y. Chi, K.F. Cen, Low-temperature gasification of waste tire in a fluidized bed, Energy Convers. Manag. 49 (2008) 2078, https://doi.org/10.1016/J.ENCONMAN.2008.02.016. –2082.

[24] J.A. Conesa, I. Martín-Gullón, R. Font, J. Jauhiainen, Complete study of the pyrolysis and gasification of scrap tires in a pilot plant reactor, Environ. Sci. Technol. 38 (2004) 3189–3194, https://doi.org/10.1021/ES034608U.

[25] V. Esmaeili, J. Ajalli, A. Faramarzi, M. Abdi, M. Gholizadeh, Gasification of wastes: the impact of the feedstock type and co-gasification on the formation of volatiles and char, Int. J. Energy Res. 44 (2020) 3587–3606, https://doi.org/10.1002/ER.5121.

[26] D. Geldart, Types of gas fluidization, Powder Technol. 7 (1973) 285–292, https://doi.org/10.1016/0032-5910(73)80037-3.

[27] P.C. Carman, Fluid flow through granular beds, Trans. Inst. Chem. Eng. 15 (1937) 150–166. https://ci.nii.ac.jp/naid/10003392892/. (Accessed 26 December 2021).

[28] J. Sánchez-Prieto, A. Soria-Verdugo, J.v. Briongos, D. Santana, The effect of temperature on the distributor design in bubbling fluidized beds, Powder Technol. 261 (2014) 176–184, https://doi.org/10.1016/J.POWTEC.2014.04.035.

[29] R. Zwart, S. van del Heijden, R. Emmen, J.D. Bentzen, P. Stoholm, J. Krogh, Tar Removal from Low-Temperature Gasifiers, 2010.

[30] D. Serrano, M. Kwapinska, A. Horvat, S. Sánchez-Delgado, J.J. Leahy, Cynara cardunculus L. gasification in a bubbling fluidized bed: the effect of magnesite and olivine on product gas, tar and gasification performance, Fuel 173 (2016) 247–259, https://doi.org/10.1016/J.FUEL.2016.01.051.

[31] M.F. Laresgoiti, I. de Marco, A. Torres, B. Caballero, M.A. Cabrero, M.J. Chomón, Chromatographic analysis of the gases obtained in tyre pyrolysis, J. Anal. Appl. Pyrol. 55 (2000) 43–54, https://doi.org/10.1016/S0165-2370(99)00073-X.

[32] J. Dodds, W.F. Domenico, D.R. Evans, L.W. Fish, P.L. Lassahn, W.J. Toth, Scrap tyres: a resource and technology evaluation of tyre pyrolysis and other selected alternative technologies, Report EGG- 2241 (1983).

[33] R. Cypres, B. Bettens, Pyrolysis and Gasification, Elsevier Applied Sciences, Barking, UK, 1989.

[34] P.T. Williams, D.T. Taylor, Aromatization of tyre pyrolysis oil to yield polycyclic aromatic hydrocarbons, Fuel 72 (1993) 1469–1474, https://doi.org/10.1016/0016-2361(93)90002-J.

[35] S. Li, I. Cañete Vela, M. Järvinen, M. Seemann, Polyethylene terephthalate (PET) recycling via steam gasification - the effect of operating conditions on gas and tar composition, Waste Manag. 130 (2021) 117–126, https://doi.org/10.1016/J.WASMAN.2021.05.023.

[36] M. Policella, Z. Wang, K.G. Burra, A.K. Gupta, Characteristics of syngas from pyrolysis and CO2-assisted gasification of waste tires, Appl. Energy 254 (2019), 113678, https://doi.org/10.1016/J.APENERGY.2019.113678.

[37] W. Xuan, H. Wang, S. Yan, D. Xia, Exploration on the steam gasification mechanism of waste PE plastics based on ReaxFF-MD and DFT methods, Fuel 315 (2022), 123121, https://doi.org/10.1016/J.FUEL.2021.123121.

[38] C. Franco, F. Pinto, I. Gulyurtlu, I. Cabrita, The study of reactions influencing the biomass steam gasification process☆, Fuel 82 (2003) 835–842, https://doi.org/10.1016/S0016-2361(02)00313-7.

[39] A. Soria-Verdugo, L. von Berg, D. Serrano, C. Hochenauer, R. Scharler, A. Anca-Couce, Effect of bed material density on the performance of steam gasification of biomass in bubbling fluidized beds, Fuel (2019) 257, https://doi.org/10.1016/j.fuel.2019.116118.